Building Complex Two− Dimensional Structures: Methylene Blue on Self-Assembled Monolayer−Covered Au(111)

C. Vericat, F. Remes Lenicov, S. Tanco, G. Andreasen, M. E. Vela, and R. C. Salvarezza*

Instituto de Investigaciones Fisicoquímicas Teóricas y Aplicadas (INIFTA), Universidad Nacional de La Plata−CONICET, Sucursal 4, Casilla de Correo 16, (1900) La Plata, Argentina

Received: April 18, 2002; In Final Form: July 2, 2002

The charge transfer of methylene blue molecules immobilized on different monolayer covered-Au(111) surfaces has been studied by electrochemical techniques complemented by scanning tunneling microscopy. The positively charged methylene blue ions (MB^+) are effectively immobilized on negatively charged S and I adlayers. The amount of charge related to the (MB^+/MBH) surface redox couple (q_{surf}) depends on the surface concentration of the adsorbed S and I atoms and on their geometric arrangement. When methylene blue immobilization is made on COO^--terminated thiols (mercaptopropionic acid, MPA, and mercaptoundecanoic acid, MUA), the value of q_{surf} is markedly reduced, indicating that the electron transfer through hydrocarbon chains is very difficult, although the MB^+ is effectively immobilized. Sulfide contamination introduces defects in the MPA and MUA layers and, thus, markedly increases the number of immobilized methylene blue molecules that are active for charge transfer. Electrochemical runs made with methylene blue in solution demonstrate that defects are the main path for electron transfer through COO^--terminated thiol-covered Au(111) surfaces. For low-defect COO^--terminated thiol adlayers, a diode-like effect related to the blocking of the anion-transport through small pores with negatively charged gates is observed.

Introduction

The use of molecules and macromolecules immobilized on self-assembled monolayers on metals has proven to be an effective route for the control of the surface chemistry in different applications such as chemical sensors,[1a] biosensors,[1b] and optoelectronic and photoelectrochemical devices[1c] and also in the field of heterogeneous catalysis[1d]. The development of nanotechnology demands selective surface covering procedures at the level of the monolayer in order to build nanominiaturized devices or structures. In most cases, molecules are immobilized on self-assembled monolayers of positively or negatively charged thiols on metallic substrates, with Au being the most studied system.[2] The electron transfer between immobilized molecules and the metallic substrate is a key point in the development of chemical sensors or biosensors.

The study of the electron transfer through self-assembled monolayers of thiols (SAMs) on metals for different redox couples has attracted considerable interest in recent years.[3−4] In the case of redox couples in solution, such as hexacyanoferrate, viologen, and ferrocene, it has been reported that the blocking capability of SAMs on a Au substrate for the electron transfer to/from different species increases as the alkanethiol hydrocarbon chain length is increased.[5] It has been shown that, for monolayer films sufficiently free from pinhole defects, where redox species are effectively blocked from the electrode surface, the dominant mechanism of electron transfer is electron tunneling through the monolayer film, a process that depends on the hydrocarbon chain length.[6] On the other hand, it has been shown that for defect-containing monolayers electron transfer takes place through pinholes or collapse sites in the monolayer, these two being the most important kinds of defects. Because defect density in the monolayer decreases with increasing hydrocarbon chain length (due to the increase in the van der Waals and hydrophobic forces acting at SAMs),[7] redox species are more effectively blocked in the case of long alkanethiols. This mechanism has been proposed in the case of copper electrodeposition on alkanethiolate-covered Au(111)[8] and for mixed SAMs of controlled composition that act as nanoporous organic surfaces.[9−10] Also, a crucial point is to determine if the electron transfer takes place at the monolayer solution interface, within the monolayer, or in direct contact with the metal surface.[3,6a] Redox couples can also be immobilized on the monolayers by different methods including covalent attachment, physisorption, and also the hydrophobic effect.[11] Immobilized redox couples such as azurin,[12] cytochrome *c*,[13] and SAMs of thiols with pendant redox centers, such as ferrocene, on Au[14] have been extensively studied because of the interest in the mechanisms of charge transfer through organic films that mimic biological membranes.

The methylene blue molecule has attracted considerable interest because it is an electron mediator between enzymes and substrates because of its characteristic redox couple:[15]

$$2e + MB^+ + H^+ \leftrightarrow MBH \qquad (1)$$

where MB^+ and MBH stand for the oxidized (cationic) and reduced (leuco) forms of methylene blue, respectively. The positive charge of the cationic form is mainly located on the S atom.[16]

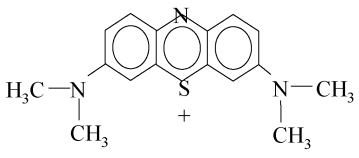

Because of its redox behavior, methylene blue has also been proposed as a sulfur sensor of the type required for electro-

* To whom correspondence should be addressed.

10.1021/jp0210071 CCC: $22.00
Published on Web 08/07/2002

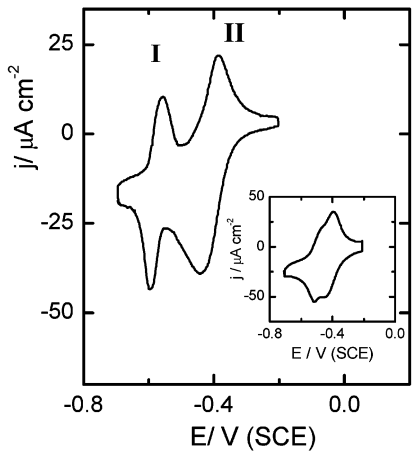

Figure 1. Typical j vs E profiles recorded at 0.05 V s^{-1} showing the MB^+/MBH redox couples for a S-covered Au(111) electrode in the 10^{-4} M MB^+-containing solution. Peak I corresponds to the immobilized MB^+, and peak II corresponds to MB^+ in solution. The S-covered Au was prepared by the traditional method, that is, by immersion of the Au(111) substrate in 3×10^{-3} M Na_2S + 0.1 M NaOH (open circuit, S_8-covered Au). The inset shows a similar j vs E profile, recorded for a bare Au electrode.

chemical−optical devices, as a means of generating singlet oxygen that causes damage in biological systems (like DNA) and, when polymerized on noble metals, as a conductive polymer with bioelectrochemical activity.[15a,17] It has been reported[18] that immersion of a Au electrode previously covered with sulfur in a diluted solution containing the cationic form of methylene blue, MB^+, leads to the formation of a surface layer that is hardly detected on bare Au (Figure 1 and inset). The reversible redox couple for this surface layer (peaks I in Figure 1) is shifted $\Delta E \approx 0.15$ V in the negative direction with respect to that of methylene blue molecules in solution (peaks II). This separation has been taken as an evidence for the formation of a disulfide bond between an adsorbed S atom and the S atom of methylene blue,[16a,18] although immobilization by electrostatic interactions between the positively charged MB^+ ion and the negatively charged S monolayer cannot be discarded. If electrostatic interactions dominate immobilization, then MB^+ could also be immobilized on COO^--terminated thiols, allowing the study of electron transfer through different hydrocarbon chains.

In this work, we have made a comparative study on the MB^+ immobilization on sulfur-, iodine-, and COO^--terminated thiol-covered Au(111) electrodes. The different negatively charged layer-covered Au substrates have been characterized by in situ STM. The amount of immobilized MB^+ molecules active for charge transfer on these layers has been followed by the charge density (q_{surf}) related to reaction 1. Results show that MB^+ ions are bounded by electrostatic forces to adsorbed negatively charged S and I adlayers. When the immobilization of methylene-blue is made on COO^--terminated thiols such as mercaptopropionic acid (MPA) or mercaptoundecanoic acid (MUA), q_{surf} is markedly reduced for MPA and negligible for MUA, although the MB^+ is effectively immobilized, as revealed by spectrophotometric experiments, thus indicating that the electron transfer is difficult through the hydrocarbon chains. Sulfide contamination introduces defects in the MPA and MUA layers and, thus, markedly increases the number of immobilized methylene blue molecules that are active for charge transfer. Electrochemical runs made with methylene blue in solution demonstrate that the dominant mechanism of electron transfer through COO^--terminated thiol monolayers is through defects. For low-defect COO^--terminated monolayers, a diode-like effect related to the blocking of the anion-transport through small pores with negatively charged gates is found.

Experimental Section

Au substrates were 1 cm^2 Au coated glass (AF 45 Berliner Glass KG, Germany) prepared by evaporation. The substrates were annealed in a hydrogen flame for 3 min. As observed by STM and AFM, these Au electrodes exhibit atomically smooth (111) terraces separated by monatomic steps in height.[19]

Solutions were prepared by using analytical grade chemicals and Milli-Q water. The MB^+-containing solutions were prepared from its chloride salt. MB^+ immobilization on negatively charged monolayer-covered Au substrates was done as follows.

(i) S-Covered Substrates. Au substrates were immersed in 3×10^{-3} M Na_2S + 0.1 M NaOH saturated with nitrogen for 10 min at open circuit potential, transferred to an electrochemical cell containing 0.1 M NaOH, and then polarized at $E = -0.55$, -0.80, and -1.10 V to form S_8-covered, $\sqrt{3} \times \sqrt{3}$ R30° S-covered and step decorated S Au(111) substrates, respectively.[20] After preparation, the S-covered Au(111) substrates were rinsed with Milli-Q water and then immersed for 30 min in a 10^{-4} M MB^+ + 0.1 M NaOH solution for MB^+ immobilization. Finally, the MB^+ modified S-covered Au substrate was rinsed again with water and used as the working electrode of an electrochemical cell containing 0.1 M NaOH to test the MB^+/MBH surface redox couple. The charge density involved in the redox couple (q_{surf}) is proportional to the amount of immobilized MB^+ molecules that are active for charge transfer. The steps involved in the preparation of the S-covered Au are schematically shown in Figure 2a.

(ii) I-Covered Substrates. The Au substrates were immersed in 0.1 M NaH_2PO_4 buffer (pH 5.8) + 3×10^{-3} M KI + 0.1 M Na_2SO_4 solution at open circuit for 10 min to form the $\sqrt{3} \times \sqrt{3}$ R30° I lattice.[21] After rinsing thoroughly with Milli-Q water, the I-covered substrates were immersed 30 min in a 10^{-4} M MB^+ + phosphate buffer + 0.1 M Na_2SO_4 solution (pH 5.8) for MB^+ immobilization. Finally, the MB^+ modified I-covered Au substrate was rinsed again with water and placed as the working electrode of an electrochemical cell containing the phosphate buffer + 0.1 M Na_2SO_4 to test the MB^+/MBH surface redox couple. The steps involved in the preparation of the I-covered Au are schematically shown in Figure 2b.

(iii) MPA- and MUA-Covered Substrates. The Au substrates were immersed in 10^{-4} M mercaptopropionic acid (MPA) or mercaptoundecanoic acid (MUA) ethanolic solutions during 24 h to form the $\sqrt{3} \times \sqrt{3}$ R30° lattice and related superlattices.[22] In some other cases, the MPA and MUA layers were annealed in the ethanolic solutions at 60−70 °C for 4 h to improve the order in the self-assembled monolayers.[23] Then the substrates were rinsed first with ethanol and then with water and immersed for 30 min in a 10^{-4} M MB^+ + 0.1 M NaOH solution for MB immobilization. Finally, the MB^+-modified thiol-covered Au substrates were rinsed again with water and placed as the working electrode of an electrochemical cell containing 0.1 M NaOH to test the MB^+ surface redox couple. For experiments with MB^+-containing solutions, the electrodes were rinsed with ethanol and water after the exposure to MPA or MUA solutions and then placed in the cell containing 10^{-4} M MB^+ + 0.1 M NaOH solution. The steps involved in the preparation of the MPA- and MUA-covered Au are schematically shown in Figure 2c.

Electrochemical measurements were performed in a conventional glass-made cell using a large Pt plate and a saturated

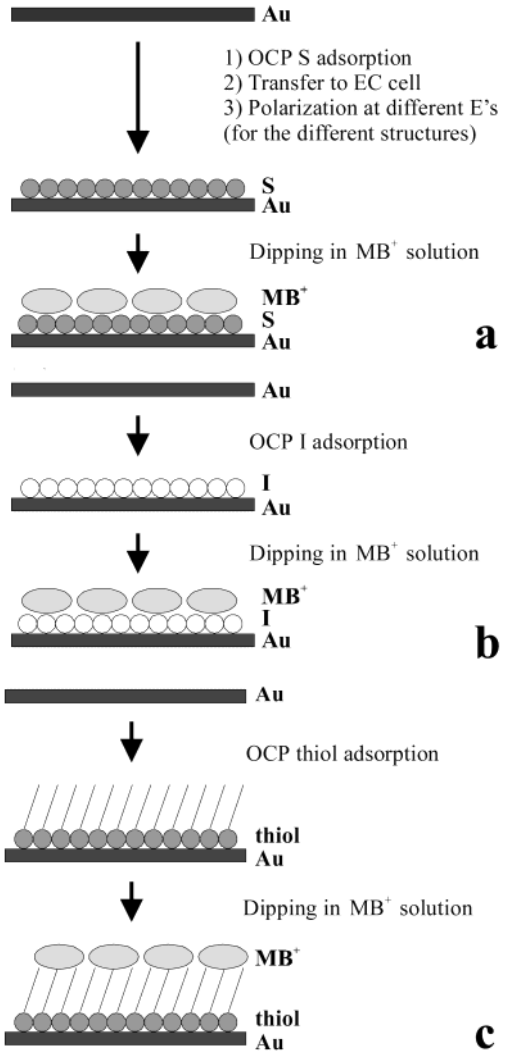

Figure 2. Scheme showing the procedure for the preparation of the different adlayers. (a) S, (b) I, and (c) COO^--terminated alkanethiols (MPA, MUA). Note that the molecules are not in scale.

calomel electrode as counter electrode and reference electrodes, respectively.

UV−visible spectra were performed on a Cary 3 (VARIAN) spectrophotometer, using a program for smoothing and averaging signals. Measurements were made using quartz cells of 1 cm optical length.

In situ STM images were obtained by using a Nanoscope III EC-STM from Digital Instruments Inc. Images were taken in the constant current mode. Typical set point currents and bias voltages were 10−20 nA and 0.3−0.6 V, respectively. Commercial Pt−Ir nanotips covered with Apiezon wax for insulation were used for STM imaging. A large area Au counter electrode and a Pd/H_2 reference electrode were used in the STM electrochemical cell, and the Au(111) substrates were used as working electrodes. All potentials in the text are referred to the saturated calomel electrode (SCE).

Results and Discussion

The *j*/*E* profile (Figure 3) recorded at a scan rate $\upsilon = 0.05$ V s^{-1} for Au(111) in 3×10^{-3} M $Na_2S + 0.1$ M NaOH shows at $E < -1.15$ V a cathodic current related to the hydrogen evolution reaction.[20] The *j*/*E* profile also shows two humps at −1.13 (AI) and −1.17 V (CI), and then two well-defined peaks at −0.90 (AII) and −0.96 V (CII). Humps AI/CI correspond to

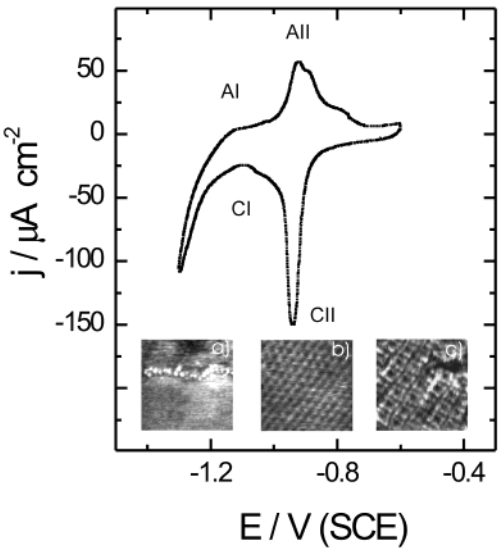

Figure 3. Typical *j* vs *E* profiles for Au electrodes recorded at 0.05 V s^{-1} in 0.1 M NaOH + 3×10^{-3} M Na_2S. The insets show the surface structures observed at different potential regions. (a) 7.5×7.5 nm^2, sulfur adsorbed at step edges, $E = -1.0$ V; (b) 5×5 nm^2, $\sqrt{3} \times \sqrt{3}$ R30° sulfur lattice, $E = -0.85$ V; (c) 5×5 nm^2, S_8, $E = -0.6$ V.

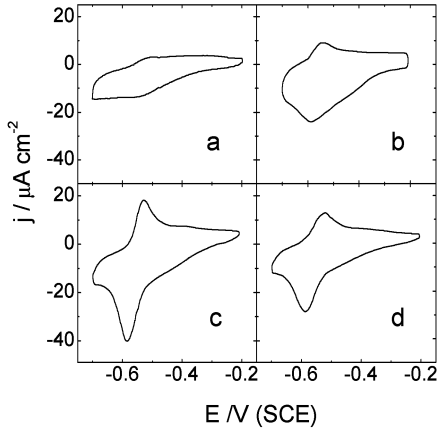

Figure 4. *j* vs *E* profile recorded at 0.05 V s^{-1} for the MB^+/MBH redox couple immobilized on different S adlayers. The electrolyte was 0.1 M NaOH. (a) Bare Au(111), (b) S decorated step-Au(111), (c) $\sqrt{3} \times \sqrt{3}$ R30° S-covered Au(111), and (d) S_8-covered Au(111).

the adsorption/desorption of S atoms at/from step edges (Figure 3a). Peak AII corresponds to the adsorption of sulfur species at terraces to form a $\sqrt{3} \times \sqrt{3}$ R30° lattice on Au(111) (Figure 3b).[20,24] This lattice is desorbed at CII. Finally, at potentials slightly more positive than −0.6 V the anodic *j* value increases due to the formation of adsorbed polymeric S species such as S_8 (Figure 3c).[20,24] The latter are reduced at ≈ -0.80 V. The S coverage (θ) changes from 1/3 to 2/3 on going from the $\sqrt{3} \times \sqrt{3}$ R30° lattice to S_8 adsorbed species.

We have thus prepared step-decorated S Au(111), $\sqrt{3} \times \sqrt{3}$ R30° S-covered Au(111) and S_8-covered Au(111) substrates by holding them at a constant potential within the potential region where these surface structures are formed. After immobilization of MB^+ and careful rinsing with water, the S-covered substrates were placed in the electrochemical cell containing 0.1 M NaOH. Voltammetric results for the different S-covered electrodes (Figure 4b−d) are compared to those obtained for a S-free Au(111) electrode subjected to the same procedure (Figure 4a). For S-free MB^+-covered Au(111), a reversible redox couple with a small charge density $q_{surf} = 5$ μC cm^{-2} is observed at $E_{redox} = -0.5$ V indicating that a small amount of MB^+ is

adsorbed on the bare Au(111) surface. For step-decorated S Au(111) electrodes (Figure 4b), the potential of the redox couple is shifted to $E_{redox} = -0.55$ V, whereas the q_{surf} value increases slightly with respect to that observed for the S-free Au(111) electrode, as expected for the low S coverage, which depends on the step density of the Au(111) substrate. On the other hand, for the $\sqrt{3} \times \sqrt{3}$ R30° S-covered Au(111) electrode ($\theta = 1/3$, S−S distance ≈ 0.5 nm; Figure 4c), the value of q_{surf} increases to 50 μC cm^{-2} and E_{redox} remains at −0.55 V. From this value, the MB^+ surface concentration results in $\Gamma = 2.5 \times 10^{-10}$ moles cm^{-2}, that is 1/3 of the $\sqrt{3} \times \sqrt{3}$ R30° surface concentration ($\Gamma = 7.6 \times 10^{-10}$ moles cm^{-2}). Considering the size of the methylene blue molecule, this means that a close packed layer of immobilized MB^+ is formed, as each MB^+ blocks three S atoms. Note that all of the molecules in the close packed MB^+ layer are active for charge transfer. However, for the S_8-covered Au(111) samples, q_{surf} decreases to 36 μC cm^{-2}, despite the larger S coverage value (θ =2/3, S−S distance $\approx$ 0.3 nm) (Figure 4d). This could reflect a more difficult MB^+ immobilization on the S_8 units and also a decrease in the $MB^+/S^{-\delta}$ interaction, with δ being the charge remaining on the S atom after adsorption. The presence of a negative charge on S is revealed by XPS measurements of S-covered electrodes.[25] In fact, the S $2p_{3/2}$ BE is shifted from the 164 eV value (corresponding to bulk S) to 161−162 eV. This shift clearly indicates a sulfide-like bond in the adlayer, in agreement with theoretical calculations.[26] Correlations between BE and charge density on the S atom[27] show that the obtained BE values correspond to partially reduced sulfur species. The decrease in q_{surf} as the applied potential is increased could be related to the fact that the value of δ in the $\sqrt{3} \times \sqrt{3}$ R30° S lattice should be higher than that in a layer of S_8 species[25] because the negative charge of adsorbed anions decreases as the potential applied to the interface is made more positive.[28,29]

In 0.1 M NaOH, the immobilized MB^+/MBH redox couple on the S-covered Au(111) electrodes exhibits a linear peak current (i_p) vs sweep rate (υ) dependence, whereas the peak potential remains independent of υ, that is, a behavior consistent with a charge-transfer controlled surface process is observed. The splitting of the anodic and cathodic peaks is $\approx$ 0.060 V, as it has been already reported[15−18,30]. Considering that on bare gold this splitting is only 0.030 V, it seems that adsorbed S atoms layer would introduce a certain degree of irreversibility to the charge-transfer process. Repeated potential cycling produces a decrease in the q_{surf} value because the MBH formed in the negative scan is desorbed from the S-covered Au(111) surface. The fact that the peak potential related to the $\sqrt{3} \times \sqrt{3}$ R30° S stripping is the same for a MB^+ immobilized S-covered electrode and for a plain S-covered electrode supports the idea that the MBH is completely desorbed from the surface before the S layer is electrodesorbed.

The contribution of electrostatic forces is also suggested by the fact that MB^+ is also immobilized on I-covered Au(111) electrodes. The typical *j*/*E* profile (Figure 5a) for a Au(111) electrode in contact with a IK containing solution shows at −0.5 V a peak (AI) corresponding to the adsorption of the iodide ions to form the $\sqrt{3} \times \sqrt{3}$ R30° lattice on Au(111) [21] (inset in Figure 5a). On the other hand, peak CI corresponds to the desorption of iodine from the $\sqrt{3} \times \sqrt{3}$ R30° lattice. After MB^+ immobilization on $\sqrt{3} \times \sqrt{3}$ R30° I-covered Au(111) substrates ($\theta = 1/3$; I−I distance $\approx$ 0.5 nm) and careful rinsing with water, voltammetric runs using these electrodes in a phosphate buffer +0.1 M Na_2SO_4 solution (pH 5.8) reveal a MB^+/MBH redox couple with $q_{sur} = 45$ μC cm^{-2} and a peak splitting of 60 mV,

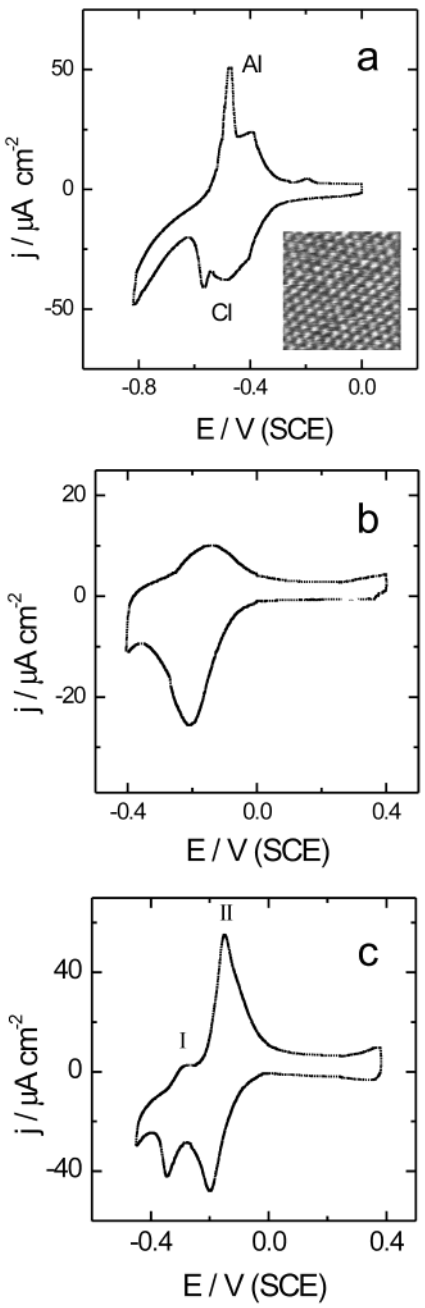

Figure 5. (a) Typical *j* vs *E* profiles for Au(111) electrode recorded at 0.05 V s^{-1} in a 3×10^{-3} M KI phosphate buffer + 0.1 M Na_2SO_4 solution (pH 5.8). Peak AI corresponds to the formation of the $\sqrt{3} \times \sqrt{3}$ R30° I lattice. Peak CI corresponds to I desorption from this lattice. The inset shows a 5 × 5 nm^2 STM image of the $\sqrt{3} \times \sqrt{3}$ R30° I lattice on Au(111), $E = -0.3$ V. (b) *j* vs *E* profile for the MB^+/MBH redox couple immobilized on a $\sqrt{3} \times \sqrt{3}$R30° I-covered Au(111) substrate. The electrolyte was a phosphate buffer +0.1 M Na_2SO_4 solution (pH 5.8). (c) *j* vs *E* profile showing the MB^+/MBH redox couples for a I-covered Au(111) electrode in a 10^{-4} M MB^+ + phosphate buffer + 0.1M Na_2SO_4 solution (pH 5.8). Peak I corresponds to the immobilized MB^+, and peak II corresponds to MB^+ in solution.

comparable to those observed for MB^+ immobilized on the $\sqrt{3} \times \sqrt{3}$ R30° S (Figure 5b). Thus, a close-packed layer of MB^+ is formed on the I-covered Au(111) electrode, with all these molecules being active for charge transfer. Note, however, that as observed for the S-covered electrodes the charge transfer through this layer seems to be more irreversible than that observed on bare gold. Also, it was necessary to lower the pH

to distinguish between peaks corresponding to iodine adsorption/desorption and MB^+/MBH redox couple. Theoretical calculations have shown that the adsorbed S atom in the $\sqrt{3} \times \sqrt{3}$ R30° lattice on Au(111) has a negative charge, $\delta = 0.4$,[26] whereas for the adsorbed I atom in the same lattice and substrate, the negative charge is $\delta = 0.1$.[21] In addition, XPS and LEED data for I^--covered electrodes have shown that in the $-0.4/-0.2$ V range, the potential range of the MB^+/MBH couple, the $\sqrt{3} \times \sqrt{3}$ R30° I lattice coexists with coadsorbed cations,[29] thus proving that a small negative charge remains on the I atoms. Also, in the case of Pt/I layers in IK, it has been reported that K^+ adsorbs in the potential range corresponding to the $\sqrt{3} \times \sqrt{3}$R30° I adlayer, thus revealing that I has a negative charge density.[31] When MB^+ is present in solution, we have observed $\Delta E = 0.15$ V for I-covered Au(111) electrodes (Figure 5c), i.e., the same ΔE value between the surface and solution redox couple observed for S-covered Au(111) (Figure 1) that has been assigned to the formation of a disulfide bond.[16a,18] However, the formation of a chemical bond cannot be invoked in the case of MB^+ immobilized on I-covered Au(111) electrodes.[32] Therefore, our experimental results show that electrostatic interactions are involved in the immobilization of MB^+ on I- and S-covered electrodes; that is, a disulfide bond is not needed for immobilization, in contrast to earlier suggestions found in the literature.[16a,18] The lack of S−S bands in the spectroscopic data of this system[30] supports the idea that no specific chemical bonds are present in this surface structure.

To understand the role of the hydrocarbon chains in the electron transfer, we have compared the behavior of the immobilized MB^+/MBH redox couple on $\sqrt{3} \times \sqrt{3}$ R30° S-covered and on $\sqrt{3} \times \sqrt{3}$ R30 °COO^--terminated thiol-covered Au(111). A comparison between these systems is attractive and valid because COO^--terminated alkanethiols self-assemble on Au(111) with S atoms also bounded to the Au atoms, with $\delta = 0.2$,[26] and negatively charged carboxylate groups facing the electrolyte solution in alkaline media.[22] In principle, if we consider the electrostatic nature of the MB^+/adsorbed layer interaction, one should expect that the net negative charge remaining in the COO^--terminated thiol layer would favor a better MB^+ immobilization for these cases than for the $\sqrt{3} \times \sqrt{3}$ R30° S-covered Au electrode. Therefore, the behavior of the MB^+/MBH redox couple, charge, and degree of reversibility should give information about the electron transport through the hydrocarbon chains, the location of the immobilized molecules and the immobilized molecule/thiol interactions. We have prepared MPA and MUA layers on Au(111) by immersion of the Au(111) substrate for 24 h in MPA- or MUA-containing ethanolic solutions. The presence of the self-assembled MPA and MUA layers was tested by recording the electrodesorption curves in 0.1 M NaOH (Figure 6a) and by STM (inset in Figure 6a). The MPA- and MUA-covered Au(111) substrates were then immersed in MB^+-containing 0.1 M NaOH solution. After careful rinsing of these samples, the voltammetric runs recorded in 0.1 M NaOH show the MB^+/MBH redox couple at $E_{redox} = -0.4$ V for MPA with a small charge, $q_{surf} = 2.5\ \mu C\ cm^{-2}$ (Figure 6b), and no traces of it for MUA. In the second case we were able to detect the redox couple at $E_{redox} = -0.4$ V only when the self-assembly process of MUA on Au(111) was made for very short times, i.e., 15 s (Figure 6c). In principle, it could be argued that MB^+ is desorbed from the monolayer because of the high ionic strength (0.1 M NaOH) of our electrolyte. However, incubation of MPA- covered Au electrodes in MB^+ solutions of lower ionic strength (0.001 M NaOH) and subsequent voltammetric runs

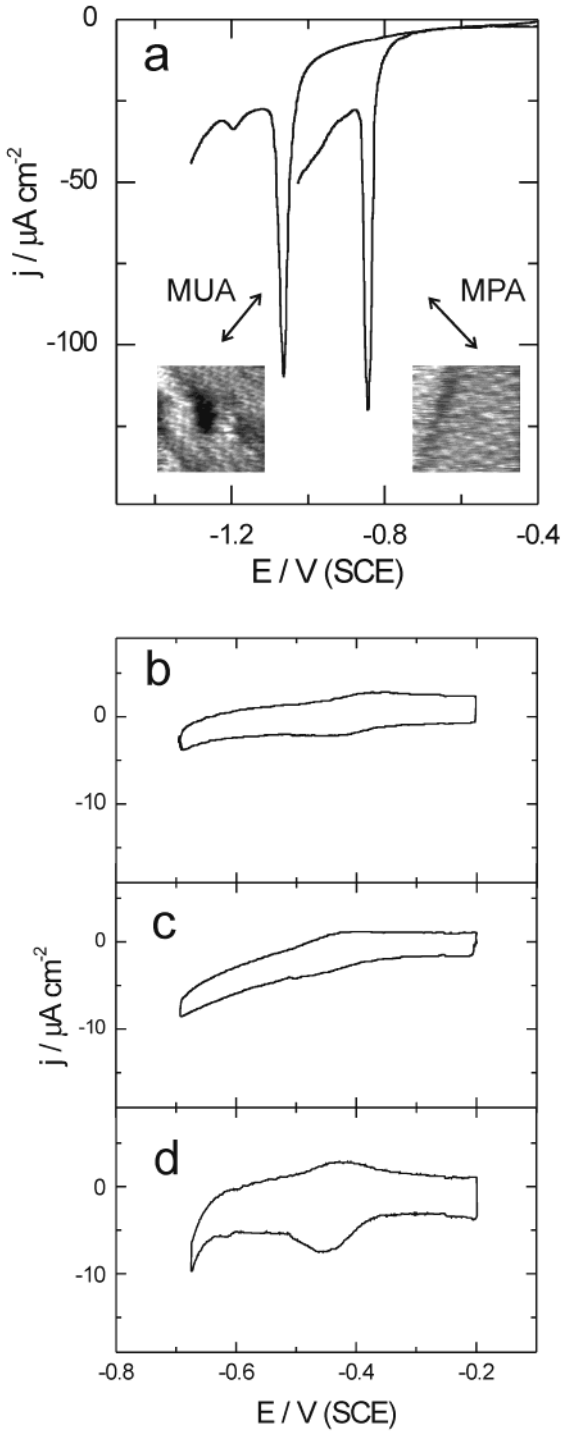

Figure 6. (a) Electrodesorption curves for MPA- and MUA-covered Au(111) electrodes recorded at 0.05 V s^{-1} in 0.1 M NaOH. The insets show MPA and MUA domains of the $\sqrt{3} \times \sqrt{3}$ R30° lattice and its related c(4 × 2) superlattice. (b) *j* vs *E* profile recorded at 0.05 V s^{-1} in 0.1 M NaOH for the MB^+/MBH redox couple immobilized on the $\sqrt{3} \times \sqrt{3}$ R30° MPA-covered Au(111) substrate. The immersion time of the Au(111) substrate in the MPA containing ethanolic solution was 24 hs. (c) *j* vs *E* profile recorded at 0.05 V s^{-1} in 0.1 M NaOH for the MB^+/MBH redox couple immobilized on the $\sqrt{3} \times \sqrt{3}$ R30° MUA-covered Au(111) substrate. The immersion time of the Au(111) substrate in the MUA containing ethanolic solution was 15 s. (d) *j* vs *E* profile recorded at 0.05 V s^{-1} in 0.1 M NaOH for the MB^+/MBH redox couple immobilized on a S-contaminated $\sqrt{3} \times \sqrt{3}$ R30° MPA-covered Au(111) substrate. The Au(111) substrate was immersed in the MPA containing ethanolic solution with traces of sulfide (5×10^{-6} M) for at least 24 h.

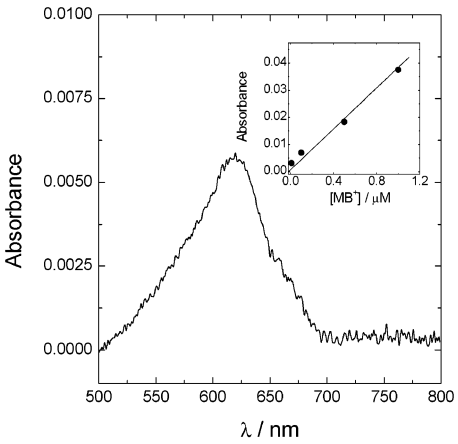

Figure 7. Spectrum of MB^+ molecules in 0.1 M NaOH electrolyte after electrodesorption from a high area MPA-covered Au electrode. The blank spectrum (a very diluted MPA solution in 0.1 M NaOH) has been subtracted. The total amount of MB^+ was estimated from the calibration curve shown in the inset for the MB^+ peak at ≈600 nm, after subtraction of the blank spectrum.

in the same electrolyte show that the charge of the surface couple q_{surf} is scarcely affected by the ionic strength.

It could be also argued that MB^+ is really not immobilized on the negatively charged MPA and MUA-covered Au(111) substrates. To address this point, we have made spectrophotometric experiments after the electrodesorption of MB^+ from a high area MPA-covered polycrystalline Au electrode. The high area polycrystalline Au electrode (roughness factor = 10; real area = 3.70 cm^2) was prepared as described previously[33] and stabilized for 24 h in order to exhibit a preferred Au(111) orientation. This electrode was covered with MPA and then immersed in the MB^+-containing solution for immobilization. The electrode was rinsed by the usual procedure and placed in a 4.0 mL electrochemical cell with 0.1 M NaOH. The potential was then scanned from −0.2 to −1.4 V at $\upsilon = 0.05$ V s^{-1} to remove the immobilized MB^+-MPA layer from the Au surface. From the recorded cathodic scan, a small value of q_{surf} (≈2.5 μC cm^{-2}) was obtained, in agreement with that measured for the immobilized MB^+-MPA-covered Au(111) electrode (Figure 6b). Finally, the potential was held at −1.4 V for 10 min to ensure the complete removal of the MB^+ -MPA layer, and the electrode was taken out from the solution at controlled potential to avoid readsorption. Then the UV− visible spectra of the solution were taken.[34] The total amount of electrodesorbed MB^+ molecules was estimated from a calibration curve (using Beer's law) for the MB peak at ≈600 nm, after subtraction of the blank spectrum (a very diluted MPA solution in 0.1 M NaOH). From the absorbance of the maximum (A≈ 0.006) and by using the calibration curve (Figure 7), a MB^+ surface concentration of 1.6×10^{-10} mole cm^{-2} can be calculated. This coverage is more than 10 times greater than that obtained from voltammetric scans for the inmobilized redox couple ($\Gamma = 1.3 \times 10^{-11}$ moles cm^{-2}). We have repeated the experiment to ensure reproducibility and have obtained similar results. Thus, we have confirmed that only a small fraction of the MB^+ molecules immobilized on the MPA-covered Au electrode are electrochemically active. In fact, our result indicates that most of the immobilized MB^+ can neither be reduced nor reoxidized because of hindered electron transfer through the hydrocarbon chains; that is, MB should have an extremely slow rate constant for the charge transfer.

To assess the role of the electrostatic forces in the immobilization process, we have performed another experiment, identical to that previously described but using a high area dodecanethiol-covered Au electrode instead of a MPA-covered Au. In this case, the UV−visible spectra of the solution remaining after the electroreduction scan does not exhibit any trace of MB^+. Thus, we have confirmed the electrostatic nature of the interaction between the MPA-Au electrodes and the MB^+ and have also showed that hydrophobic forces between the neutral hydrocarbon tail of dodecanethiol and the hydrophobic part of MB^+ molecule do not play an important role in the immobilization process.

Now we will refer to the small amount of electrochemically active MB^+ molecules. The density of electroactive molecules derived from our q_{surf} value (≈6×10^{12} molecules cm^{-2}) is close to the average defect density (≈10^{12} defects cm^{-2}) reported for thiol monolayers from in situ STM imaging.[35] Therefore, it is reasonable to think that in the case of MB^+ electroactive molecules are only those immobilized in defects of the thiol layers. The fact that the MB^+ surface redox couple is equally reversible for MPA and MUA supports the defect mechanism, discarding electron tunneling through the thiol layer. The splitting of the anodic and cathodic peaks for the MB^+/MBH on MPA or MUA- covered Au(111) electrodes is ≈ 0.030 V, as found on bare gold. However, the MB^+ redox couple on the Au surface has $E_{redox} = -0.52$ V (Figure 4a), whereas the surface MB^+/MBH redox couple on MPA- and MUA- covered Au(111) appears at $E_{redox} = -0.41$ V. This change in the potential of the redox couple could be caused by partial penetration of MB^+ molecules in defects[12] or because the different local environment (given by the hydrocarbon chains) would affect the formal potential of MB^+ molecules in direct contact with the electrode.[36] However, the important fact is that the MB redox couple seems to require a strong electronic coupling between methylene blue molecules and the adsorbed species. This is the case in S- or I-coated monolayers but not in thiol- covered adlayers, where the electron transfer can only proceed through defects.

Taking into account the present scenario, it should be possible to increase the number of immobilized methylene blue molecules active for charge transfer by introducing nanometer-sized domains of S in the MPA self-assembled monolayer. We have therefore added traces of sulfide (5×10^{-6} M) to the ethanolic solution used for MPA self-assembly because this is expected to promote the formation of S domains because of the competition of both adsorbates for the Au(111) surface. When an electrode prepared in this way was immersed in the 10^{-4} M MB^+ + 0.1 M NaOH solution, the potential of the MB^+/MBH redox couple decreased slightly to −0.45 V, whereas the q_{surf} value increased five times (Figure 6d) with respect to the electrodes formed from sulfide-free ethanolic solutions (Figure 6b). We have also verified that the electrodesorption peak potential corresponding to MPA (Figure 6a) remains at −0.84 V; that is, we have prepared a sulfide-contaminated MPA layer rather than a composite MPA−sulfide or a simple sulfide layer. In fact, note that the electrodesorption of the $\sqrt{3} \times \sqrt{3}$ R30° S layer takes place at −0.93 V, as shown in Figure 3. The introduction of small sulfide domains could be a new route to improve the performance of reactions involving mediators for charge transfer in enzyme reactions when COO^--terminated thiols are used to immobilize the enzyme.[37]

The role of defects in the thiol layer is also revealed by the behavior of the redox couple when MB^+ is present in the solution. As mentioned before, the peaks shown in Figure 8a,b, also at $E_{redox} = -0.41$ V, exhibit a linear peak current (i_p) vs $\upsilon^{1/2}$ dependence, in good agreement with a diffusion controlled process. The fact that only one anodic and one cathodic peak

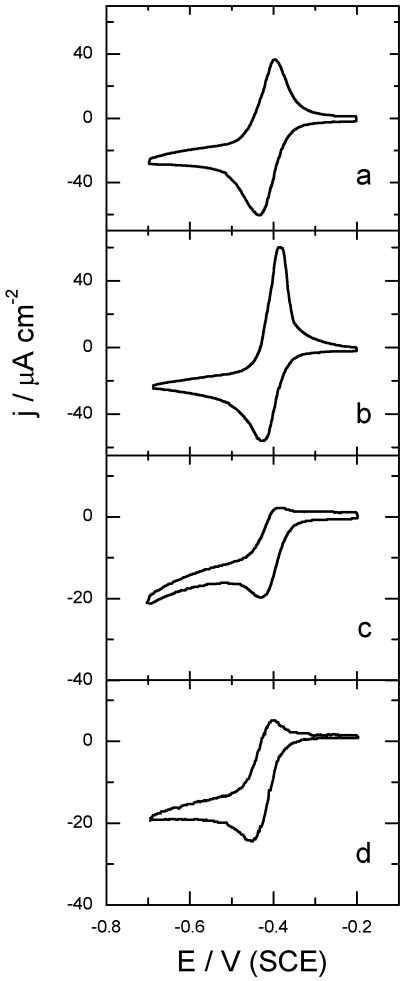

Figure 8. Typical j vs E profiles recorded at 0.05 V s^{-1} showing the MB^+/MBH redox couples in solution for (a) MPA- and (b) MUA-covered Au(111) electrodes. Electrolyte: 10^{-4} M $MB^+ + 0.1$ M NaOH. Similar j vs E profiles recorded for annealed (c) MPA- and (d) MUA-covered Au(111) electrodes.

are observed (there is no "prewave") indicates a weak interaction between MB^+ and the MPA and MUA layers,[38] as already mentioned. The magnitude of the total charge involved in the redox couple in solution (q_{sol}) is of the same order as that observed for the noncovered Au(111), $q_{sol\ Au} = 350\ \mu C\ cm^{-2}$ (Figure 1a, inset). This results could indicate that (i) MPA and MUA layers contain a large number of defects that connect the Au(111) surface with the electrolyte allowing the direct charge transfer between the Au and the MB^+ species in solution and (ii) the electron transfer between the Au substrate and the MB^+ species in solution through the hydrocarbon chain is allowed, in contrast to that observed for the immobilized molecules. To verify the electron transfer mechanism involved in these systems, MPA- and MUA-covered Au(111) electrodes were subjected to an annealing procedure that drastically reduces the defect number in the self-assembled thiol layer.[23] This procedure involves an incubation of the Au(111) substrates at 60−70 °C from the MPA and MUA ethanolic solutions during 4 h. After careful rinsing, first with ethanol and then with water, the substrates were immersed in the 10^{-4} M $MB^+ + 0.1$ M NaOH solution. The voltammetric runs for the annealed layers shown in Figure 8c,d indicate a considerable decrease in the total charge to a value $q_{sol} \approx {}^1/_2 q_{solAu}$ or lower; that is, the q_{sol} value depends on the defect density. This, and also the fact that voltammograms at different scan rates for MB^+ in MPA- and MUA-covered monolayers are equally reversible, confirms that the redox process takes place by a mechanism involving defects[9] and not by electron tunneling.[6] This behavior, as already mentioned, has also been observed in binary SAMs consisting of a framework component (a long *n*-alkanethiol) and a template (a shorter, functionalized thiol, which induces defects).[10] Thus, we can say in general that in highly defective monolayers, i.e., those with a high surface concentration of template or, as in our case, simply assembled without annealing, an electrochemical behavior that would correspond to linear diffusion is observed, yielding voltammograms such as in Figure 8a,b with $q_{sol} \approx q_{solAu}$; that is, the diffusion layers of the defects overlap, and the whole electrode area is accessible.[9a] On the other hand, monolayers with low defect density, prepared from solutions with low concentration of template or subjected to the annealing procedure, show in their voltammograms some contribution of radial diffusion, because defects behave like an array of microelectrodes (Figure 8c,d).[9a,10] It is important to remark that self-assembled monolayers, even if samples were immersed in thiol solutions for many hours or even days, can have more defects than expected. For annealed and nonannealed monolayers, it is reasonable to think that immobilized MB^+ is an efficient "connector" that catalyzes the electron transfer between the electrode and the methylene blue molecules in solution.

Finally, and more interesting, we have noted that for the annealed samples the anodic reaction in solution is practically inhibited. The anodic charge (q^+_{sol}) is in the range ${}^1/_{50} q^+_{solAu} < q^+_{sol} < {}^1/_5 q^+_{solAu}$, whereas the cathodic counterpart displays the typical diffusion-controlled peak with $q^-_{sol} \approx {}^1/_3 q^-_{solAu}$. The inhibited oxidation of MBH to MB^+ can be associated to the hindered transport of the negatively charged counterions (OH^-) through the COO^- gates of the small pores resulting from the annealing. The hindering of this transport, necessary to maintain the electroneutrality at the interface where MB^+ ions are produced by MBH oxidation, blocks the anodic reaction leading to a diode-like behavior of the MB^+/MBH redox couple.[39] In principle, it could be argued that rapid diffusion of MBH from small isolated defects (acting as an array of microelectrodes in the annealed layer) to bulk solution could inhibit its further oxidation to MB^+. However, similar experiments made with annealed and nonannealed dodecanethiol-covered Au electrodes in the MB^+-containing solution show a similar q^+_{sol}/q^-_{sol} ratio in both situations (annealed and non- annealed), thus suggesting that the charge of the group facing the electrolyte is responsible for the diode effect. This opens the possibility of building ultrathin permselective membranes with potential applications in microanalysis and corrosion protection.

Conclusions

(1) The immobilization of MB^+ on negatively charged S- and I− covered Au(111) is dominated by electrostatic interactions.

(2) The amount of immobilized MB^+ depends on the surface concentration of the adsorbed atoms and on their geometric arrangement.

(3) The immobilization of MB^+ on $\sqrt{3} \times \sqrt{3}$ R30° S- and I-covered Au(111) substrates and the electron transfer through these layers is highly efficient.

(4) The electron transfer from the COO^--terminated thiol-covered Au(111) to the immobilized MB^+ is not efficient because a strong electronic coupling between MB and thiol molecules cannot be attained. The possible mechanism for electron transfer of immobilized MB^+ is through defects in the thiol layer.

(5) Traces of sulfide added during thiol self-assembly can be used to create defects in the adlayer and, accordingly, to improve the number of immobilized MB^+ molecules active for charge transfer. This can lead to a new route to improve the performance of reactions involving mediators for charge transfer in enzyme reactions when MPA is used to immobilize the enzyme.

(6) When MB^+ is present in the electrolyte, the main effective pathway for electron transport from the COO^--terminated thiol-covered Au(111) to the MB^+ species in solution is through defects in the thiol adlayer.

(7) For low-defect COO^--terminated and MB^+ in solution, a diode-like effect related to the blocking of the anion transport through the gate of small pores with negatively charged gates is observed. This can be used to build ultrathin permselective membranes with potential applications in microanalysis and corrosion protection.

Acknowledgment. The authors thank Agencia Nacional de Promoción Científica y Tecnológica (PICT 99-5030) and CONICET (PIP-0897) (Argentina) for the financial support of this work. M.E.V. and G.A are researchers from CIC(Argentina).

References and Notes

(1) (a) Steinberg, S.; Tor, Y.; Sabatani, E.; Rubinstein, I. *J. Am. Chem. Soc.* **1991**, *113*, 5176. Turyan, I.; Mandler, D. *Anal. Chem.* **1997**, *69*, 894. Moore, A. J.; Goldenberg, L. M.; Bryce, M. R.; Pettty, M. C.; Monkman, A. P.; Marenco, C.; Yarwood, J.; Joyce, M. J.; Port, S. N. *Adv. Mater*. **1998**, *10*, 395. Flink, S.; Boukamp, B. A.; van der Berg, A.; van Veggel, F. C. J. M.; Reinhouldt, D. N. *J. Am. Chem. Soc.* **1998**, *120*, 4652. (b) Schmidt, H.-L.; Schumann, W.; Scheller, F. W.; Schubert, F. In *Sensors-A comprehensive survey*; Göpel, W., Hesse, J., Zemel, J. N., Eds.; VCH− Verlagsgesellschaft, Weinheim, Germany, 1995; Vol. 3. Mrksich, M.; Whitesides, G. *Annu. Rev. Biophys. Biomol. Struct.* **1996**, *25*, 55. Rubin, S.; Chow, J. T.; Ferraris, J. P.; Zawodzinski, T. A. *Langmuir* **1996**, *12*, 363; Heleg-Shabtai; Katz, E.; Willner, I. *J. Am. Chem. Soc.* **1997**, *119*, 8121. Lotzbeyer, T.; Schuhmann, W.; Schmidt, H.-L. *Bioelectrochem. Bioenerg.* **1997**, *42*, 1. (c) Willner, I.; Willner, B. *Bioelectrochem. Bioenerg*. **1997**, *42*, 43. Imahori, H.; Yamada, H.; Nishimura, Y.; Yamazaki, I.; Fukuzumi, S. *Langmuir* **2001**, *17*, 4925. (d) Dressick, W. J.; Dulcey, C. S.; Georger, J. H., Jr.; Calabrese, G. S.; Calvert, J. M. *J. Electrochem. Soc*. **1994**, *141*, 210. Upadhyay, D. N.; Yegnaramon, V.; Rao, G. P. *Langmuir* **1996**, *12*, 4249. Zak, J.; Yuan, H.; Ho, M.; Woo, L. K.; Porter, M. D. *Langmuir* **1993**, *9*, 2772.

(2) Ulman, A. *Chem. Rev.* **1996**, *96*, 1533. Finklea, H. O. In *Electroanalytical Chemistry*; Bard, A. J., Rubinstein, I., Eds.; Marcel Dekker: New York, 1996; pp 109−335, Vol 19. Flink, S.; van Veggel, F. C. J. M.; Reinhouldt, D. N. *Adv. Mater*. **2000**, *12*, 1315. Finklea, H. O. In *Encyclopedia of Analytical Chemistry: Applications, Theory and Instrumentation*; Meyers, R. A., Ed.; Wiley & Sons: New York, 2000.

(3) Sagara, T.; Kawamura, H.; Nakashima, N. *Langmuir* **1996**, *12*, 4253.

(4) Rubinstein, I.; Steimberg, S.; Tor, Y.; Shanzer, A.; Sagiv, J. *Nature* **1988**, *332*, 426. Porter, M. D.; Bright, T.; Allara, D.; Chidsey, C. E. D. *J. Am. Chem. Soc.* **1987**, *109*, 3559. Rubinstein, I.; Steimberg, S.; Tor, Y.; Shanzer, A.; Sagiv, J. *Nature* **1989**, *337*, 216. Chidsey, C. E. D. *Science* **1991**, *251*, 919.

(5) Finklea, H. O.; Robinson, L. R.; Blackburn, A.; Richter, B.; Allara, D.; Bright, T. *Langmuir* **1986**, *2*, 239. Sabatani, E.; Rubinstein, I.; Maoz, R.; Sagiv, J. *J. Electroanal. Chem.* **1987**, *219*, 365. Finklea, H. O.; Snider, D. A.; Fedyk, J. *Langmuir* **1990**, *6*, 371. Chidsey, C. E. D.; Loiacono, D. N. *Langmuir* **1990**, *6*, 682.

(6) Miller, C. J.; Cuendet, P.; Grätzel, M. *J. Phys. Chem.* **1991**, *95*, 877. (b) Miller, C. J.; Grätzel, M. *J. Phys. Chem.* **1991**, *95*, 5225. (c) Becka, A. M.; Miller, C. J. *J. Phys. Chem.* **1992**, *96*, 2657. (d) Terrettaz, S.; Becka, A. M.; Traub, M. J.; Fettinger, J. C.; Miller, C. J. *J. Phys. Chem.* **1995**, *95*, 11216.

(7) Vela, M. E.; Martin, H.; Vericat, C.; Andreasen, G.; Hernandez Creus, A.; Salvarezza, R. C. *J. Phys. Chem. B* **2000**, *104*, 11878.

(8) Cavalleri, O.; Bittner, A. M.; Kind, H.; Kern, K.; Greber, T. *Z. Phys. Chem.* **1999**, *208*, 107.

(9) Sabatani, E.; Rubinstein, I. *J. Phys. Chem.* **1987**, *91*, 6663. (b) Finklea, H. O.; Snider, D. A.; Fedyk, J.; Sabatani, E.; Gafni, Y.; Rubinstein, I. *Langmuir* **1993,** *9*, 3660.

(10) Chailapakul, O.; Crooks, R. M. *Langmuir* **1993**, *9*, 884. Chailapakul, O.; Crooks, R. M. *Langmuir* **1995**, *11*, 1329.

(11) Cunningham, A. *Introduction to Bioanalytical Sensors*; Wiley-Interscience: New York, 1998.

(12) Chi, Q.; Zhang, J.; Andersen, J. E. T.; Ulstrup, J. *J. Phys. Chem. B* **2001**, *105*, 4669.

(13) Tarlov, M. J.; Bowden, E. F. *J. Am. Chem. Soc*. **1991**, *113*, 1847. Collinson, M.; Bowden, E. F.; Tarlov, M. J. *Langmuir* **1992**, *8*, 1247. Song, S.; Clark, R. A.; Bowden, E. F.; Tarlov, M. J. *J. Phys. Chem*. **1993**, *97*, 6564. Feng, Z. Q.; Imabayashi, S.; Kakiuchi, T.; Niki, K. *J. Chem. Soc. Faraday Trans.* **1997**, *93*, 1367. Clark, R. A.; Bowden, E. F. *Langmuir* **1997**, *13*, 559. El Kasmi, A.; Wallace, J. M.; Bowden, E. F.; Binet, S. M.; Linderman, R. J. *J. Am. Chem. Soc*. **1998**, *120*, 225. Avila, A. A.; Gregory, B. W.; Niki, K.; Cotton, T. M. *J. Phys. Chem. B* **2000**, *104*, 2759. Murgida, D. H.; Hildebrandt, P. *J. Phys. Chem. B* **2001**, *105*, 1578. Rivas, L.; Murgida, D. H.; Hildebrandt, P. *J. Phys. Chem. B*, **2002**, *106*, 4823.

(14) Smalley, J. F.; Feldberg, S. W.; Chidsey, C. E. D.; Linford, M. R.; Newton, M. D.; Liu, Y.-P. *J. Phys. Chem*. **1995**, *99*, 13141. Weber, K.; Hockett, L.; Creager, S. *J. Phys. Chem B* **1997**, *101*, 8286.

(15) Svetlicic, V.; Zutic, V.; Clavilier, J.; Chevalet, J. *J. Electroanal. Chem.*, **1991**, *312*, 205. (b) Liu, Y.; Qian, J.; Deng, J.; Yu, T. *Ana. Chim. Acta* **1995**, *316*, 65. (c) Han, S.; Zhu, M.; Yuan, Z.; Li, X. *Biosens. Bioelectron.* **2001**, *16*, 9.

(16) Clavilier, J.; Svetlicic, V.; Zutic, V.; Ruscic, B.; Chevalet, J. *J. Electroanal. Chem.* **1988**, *250*, 427. (b) Svetlicic, V.; Clavilier, J.; Zutic, V.; Chevalet, J.; Elachi, K. *J. Electroanal. Chem.* **1993** *344*, 145.

(17) Karyakin, A. A.; Strakhova, A. K.; Karyakina, E. E.; Varfolomeyev, S. D.; Yatsimirsky, A. K. *Bioelectrochem. Bioenerg.* **1993**, *32*, 35. Brett, C. M. A.; Inzelt, G.; Kertesz, V. *Anal. Chim. Acta* **1999**, *385*, 119. Liu, J.; Mu, S.; *Synth. Met.* **1999**, *107*, 159. Rohs, R.; Sklenar, H.; Lavery, R.; Roder, B. *J. Am. Chem. Soc.* **2000**, *122*, 2860.

(18) Zutic, V.; Svetlicic, V.; Clavilier, J.; Chevalet, J. *J. Electroanal. Chem.* **1987**, *233*, 199.

(19) Andreasen, G.; Vela, M. E.; Salvarezza, R. C.; Arvia, A. J. *Langmuir* **1997**, *13*, 6814.

(20) Andreasen, G.; Vericat, C.; Vela, M. E.; Salvarezza, R. C. *J. Chem. Phys.* **1999**, *111*, 9457. Vericat, C.; Andreasen, G.; Vela, M. E.; Salvarezza, R. C. *J. Phys. Chem. B* **2000**, *104*, 302.

(21) Gao, X.; Edens, F. J.; Liu, F.-C.; Hamelin, A.; Weaver, M. J. *J. Phys. Chem.* **1994**, *98*, 8086. Batina, N.; Yamada, T.; Itaya, K. *Langmuir* **1995**, *11*, 4568.

(22) Azzaroni, O.; Vela, M. E.; Martin, H.; Hernández Creus, A.; Andreasen, G.; Salvarezza, R. C. *Langmuir* **2001**, *17*, 6647.

(23) Bumm, L. A.; Arnold, J. J.; Charles, L. F.; Dunbar, T. D.; Allara, D. L.; Weiss, P. S. *J. Am. Chem. Soc.* **1999**, *121*, 8017.

(24) McCarley, R. L.; Kim, Y.-T.; Bard, A. J. *J. Phys. Chem.* **1993**, *97*, 211. Gao, X.; Zhang Y.; Weaver, M. J. *J. Phys. Chem*. **1992**, *96*, 4156.

(25) Vericat, C.; Vela, M. E.; Andreasen, G.; Salvarezza, R. C.; Vázquez, L.; Martín-Gago, J. A. *Langmuir* **2001**, *17*, 4919.

(26) Carro, P. Unpublished results.

(27) Lindberg, B. J.; Hamrin, G. J.; Gelius, U.; Fahlman, A.; Nordling, C.; Siegbahn, K. *Phys. Scr.* **1970,** *1*, 286−298. Bourg, M.-C.; Badia, A.; Lennox, R. B. *J. Phys. Chem. B* **2000**, *104*, 6562.

(28) Paredes Olivera, P.; Patrito, E. M.; Sellers, H. In *Interfacial Electrochemistry: Theory, Experiment, and Applications*; Wieckowski, A., Ed.; Marcel Dekker: New York, 1999; p 75.

(29) Bravo, B. G.; Michelhaugh, S. L.; Soriaga, M. P.; Villegas, I.; Suggs, D. W.; Stickney, J. L. *J. Phys. Chem.* **1991**, *95*, 5245.

(30) Barner, B. J.; Corn, R. M. *Langmuir* **1990**, *6*, 1023.

(31) Lu, F.; Salaita, G. N.; Baltruschat, H.; Hubbard, A. *J. Electroanal. Chem.* **1987**, *222*, 305.

(32) Cotton, F. A.; Wilkinson, G., *Advanced Inorganic Chemistry*; Wiley & Sons: New York, 1990.

(33) Vázquez, L.; Bartolomé, A.; Baró, A. M.; Alonso, C.; Salvarezza, R. C.; Arvia, A. J. *Surf. Sci.* **1989**, *215*, 171.

(34) Green, F. J. *The Sigma-Aldrich Handbook of Stains, Dyes and Indicators*; Aldrich Chemical Co., Inc.: Milwaukee, WI, 1990.

(35) Vericat, C.; Andreasen, G.; Vela, M. E.; Martin, H.; Salvarezza, R. C. *J. Chem. Phys.* **2001**, *115*, 6672.

(36) Finklea, H. O.; Hanshew, D. D. *J. Am. Chem. Soc.* **1992**, *114*, 3173.

(37) Dong, S.; Li, J. *Bioelectrochem. Bioenerg.* **1997**, *42*, 7. (b) Guiomar, A. J.; Guthrie, J. T.; Evans, S. T. *Langmuir* **1999**, *15*, 1198.

(38) Bard, A. J.; Faulkner, L. R. *Electrochemical Methods: Fundamental and Applications*; Wiley & Sons: New York, 1980; Chapter 12.

(39) Lipkowski, J. In *Modern Aspects of Electrochemistry*; Conway, B. E., Bockris, J. O'M., White, R. E., Eds.; Plenum Press: New York, 1992; Vol. 23, p 83.